

# Electromyography-based Intentional-Deception Behavior Analysis in an Interactive Social Context: Statistical Analysis and Machine Learning

Zizhao Dong<sup>1,2</sup>, Jingting Li<sup>\*2,3</sup>, Su-Jing Wang<sup>2,3</sup>, and Gongxiang Chen<sup>\*1</sup>

<sup>1</sup> School of Education and Psychology, University of Jinan, Jinan, 250024, China

<sup>2</sup> CAS Key Laboratory of Behavioral Science, Institute of Psychology, Beijing, 100101, China

<sup>3</sup> Department of Psychology, University of the Chinese Academy of Sciences, Beijing, 101408, China

\* Corresponding authors

**Abstract.** Lying is a common social behavior, and accurate lie detection is crucial in areas such as national security. However, existing lie detection techniques have certain limitations. Therefore, more accurate and reliable tools and methods are needed to meet the practical needs of lie detection. In this context, this study discovered the potential value of electromyography (EMG) as a lie detection indicator. Specifically, this study used EMG for statistical analysis and machine learning recognition analysis of the lying process in an interactive scenario of active lying. Furthermore, we compared the performance of two traditional machine learning models and one deep learning model for lie detection based on EMG signals. In particular, time-dimensional and time-frequency-dimensional EMG features were used to mine and lie related features. Statistical results showed that compared to truth-telling, people tend to suppress their facial expressions when preparing to lie. Some facial muscle movements that were not be successfully suppressed after lying may be crucial for detecting lies. Besides the statistic analysis, the analysis results of machine learning also demonstrated demonstrate the potential of machine learning models for EMG-based intelligent lying process analysis, particularly the RUSBoosted tree. In addition, our experiment result also proved that focusing on specific facial muscles, such as Corrugator supercillii, could improve the accuracy and efficiency of intelligent algorithms. In summary, our research results provide more insights into the cognitive and facial muscle movement patterns involved in lying based on statistical analysis and machine learning.

**Keywords:** Facial electromyography · Intentional-deception behavior · Interactive social context · Machine learning · Micro-expression.

## 1 Introduction

Lying is a common social behavior in daily life, with people lying on average one or two times per day [7]. When someone is lying, he or she may experience emotions such as fear, guilt, and excitement, which can manifest in physical responses that we maybe can use as "clues" to detect lies [12,32]. Unfortunately, despite the prevalence of lying and the manifestation of lying clues, most people have a success rate of detecting lies below or equal to 50% (random level), according to the majority of published studies [10,5,3,19,22,21].

The accuracy of lie detection is critical in fields like criminal justice, clinical medicine, and national security, where experts often achieve 80% to 90% accuracy [4]. These experts are quicker in judgment, more attuned to non-verbal cues such as facial expressions, and more sensitive to subtle emotional changes [25,33,16]. In high-stakes situations, facial muscles may involuntarily reveal genuine emotions, such as through micro-expressions [11,26,20]. Micro-expressions have been suggested as indicators for detecting lies [23]. However, detecting lies through subtle facial changes at the visual level is challenging. To address this, our study introduces electromyography (EMG) as an objective indicator to measure facial expressions. EMG signals capture facial muscle movements, allowing for the quantification of both macro-expressions and micro-expressions [1]. This method enables more accurate analysis and identification of lies.

For humans, the EMG-based lie detection analysis involves simply mapping the changes in EMG signals on the temporal or frequency domain. Nevertheless, delving deeper into the correlation between facial muscle movements and deception requires more than just basic signal processing and observation of EMG signals. This is where machine learning techniques excel, as they are capable of extracting high-level features related to deception from a large number of data [2]. In other words, machine learning could uncover subtle patterns and relationships in the data that may not be apparent to human observers. This highlights the potential of machine learning in the field of facial EMG-based lie detection.

When observing facial expressions with human vision, only the movement of muscles and changes in expressions can be observed. In contrast, small muscle activities or physiological signals cannot be visually detected. Whether it is facial expressions or micro-expressions, these behaviors fundamentally involve the movement of facial muscles. Therefore, we hypothesize that EMG signals generated by muscle movements can be used to replace visual information for analysis, leading to the same conclusions as previous research. In general, this study aims to further explore the feasibility and effectiveness of using EMG signal analysis methods to identify deceptive behavior based on existing research and to expand our understanding of deceptive behavior.

Specifically, we design a face-to-face interactive experimental paradigm with high ecological validity so as to collect EMG-based lying data. First, we identify the movement patterns of facial muscles during lying through statistical analysis based on EMG signal. Then, our study demonstrates that the system combining

EMG and machine learning can achieve intelligent lie detection by mining the physiological signal features during lying. Moreover, we refine the region-wise study of facial muscles and the phase-wise study of the lying process with the help of EMG acquisition system. In sum, these findings have the potential to enhance the development of more precise expert systems for lie detection and deepen our comprehension of the physiological and emotional processes involved in deception.

## 2 Related Works

The study of lie detection using EMG is still an emerging field and there is not much relevant research. In this subsection, we focus on reviewing related works on feature extraction and machine learning based on EMG signals, providing technical support for the intelligent lie detection analysis in this article.

Regarding feature extraction, EMG signal analysis through time domain information is an intuitive approach. Lola C and Karkar et al. increased the validity of the EMG signal by using a bandpass filter and a noise detection algorithm [14]. Nihal Fatma et al. reduced the dimensionality of the EMG signal by using principal component analysis (PCA), which aided in the computation and storage of EMG signal [15]. Anastasia Shuster et al. extracted the EMG features in the zygomaticus major and corrugator supercilii regions and applied machine learning algorithms to identify lies [30]. In addition, the importance of EMG frequency domain information is gaining attention. For example, Zawawi et al. used spectrograms to characterise the EMG signal and their experimental results proved its feasibility [35].

Regarding the machine learning, determining whether someone is lying or not is a binary classification task. For one-dimensional EMG signals, it is common to use some traditional machine learning algorithms for classification. This is because machine learning can look for patterns in data to give data-driven probabilistic predictions, and these patterns improve the interpretability of machine learning algorithms. For the binary classification problem, linear support vector machine (SVM) is a simple and effective machine learning method. Even if the sample size is relatively small, SVM can achieve good results [31]. Fricke et al. used SVM and K-Nearest Neighbors (KNN) to classify the different activities represented by EMG signals, where SVM outperforms KNN [13]. Furthermore, the dataset of truth-telling and lying samples suffers from unbalanced data distribution. However, traditional machine learning methods tend to create sub-optimal classification models when there are far more examples of one class in the training dataset than of the other classes. RUSBoost is a very simple and effective algorithm for unbalanced datasets. For example, the effectiveness of RUSBoost was validated using 15 datasets from different domains and achieved good results for all unbalanced data samples [29].

Compared to statistic-based machine learning methods, deep learning based on neural networks is well able to mine advanced features related to labels. Convolutional neural network (CNN) was applied to classify EMG signals and

achieved recognition rates of up to 67.6%, indicating the promising research approach of using deep learning for EMG signals [13]. For spectrograms, deep learning is more adequate for learning features. Joshi et al, created spectrogram images of segmented sEMG signals by means of the short time Fourier transform [17]. Ozdemir et al. collected EMG signals from arm muscles and trained a residual network (ResNet) using spectrogram to recognize seven different gestures, achieving 99.59% accuracy [24]. In summary, it is feasible to apply spectrogram images of EMG signals to lie detection using deep learning models.

### 3 Method

#### 3.1 Data acquisition

This study used a face-to-face interaction interrogation paradigm to conduct the experiment [34]. The experiment involved 22 volunteers, with a mean age of 24.59 years ( $SD = 2.99$ ). The participants were randomly paired into 11 groups, with each pair consisting of individuals who did not previously know each other.

In a face-to-face interrogation competition, participants were assigned the roles of interrogee and interrogator by alternating means. The interrogee was tasked with providing truth-telling or lying responses to the interrogator’s yes-or-no queries regarding baseline information, autobiographical information, and personal preferences. For example, "Were you born in February?", "Have you ever seen the sea?", "Do you like coffee?" etc. Furthermore, the interrogator correctly recognized that the interrogee was lying in a trial, an additional 5 CNY bonus would be awarded to the interrogator. If the interrogator failed to recognize the interrogee lying in a trial, an additional 5 CNY bonus would be awarded to the interrogee. The bonus was set to stimulate strong competitive motivation among participants to deceive each other. The detailed process is shown in Fig. 1. The whole experiment was recorded.

Meanwhile, we recorded facial EMG at a sampling frequency of 1 KHz using EMG recording equipment and silver chloride cup electrodes. Regarding the electrode distribution on the face, we selected seven locations on the left side of the face for EMG signal acquisition, including frontalis (channel 1, C1), corrugator supercilii (channel 2, C2), orbicularis oculi (channel 3, C3), levator labii superioris alaeque nasi (channel 4, C4), zygomaticus (channel 5, C5), orbicularis oris (channel 6, C6), depressor anguli oris (channel 7, C7), as illustrated in Fig. 2. Specifically, the experiment was designed with electrodes attached to the left side of the face but not the right side. This asymmetric setup allowed the interrogator to observe changes in the expression of the participant’s right face, while also capturing more pronounced facial muscle movements through electromyography, as studies have shown that the left facial region expresses emotions more strongly than the right facial region [9].

#### 3.2 Data Annotation

As mentioned in Subsection 3.1, we simultaneously recorded participants’ audio signals during the experiment. This allowed us to segment and label the

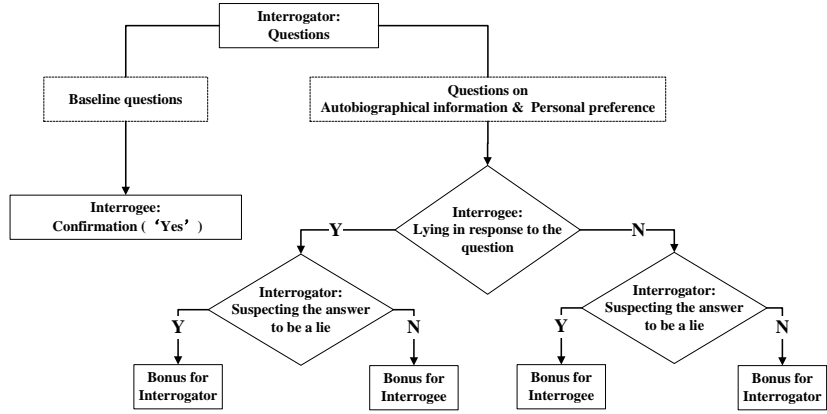


Fig. 1: Experimental procedure detail.

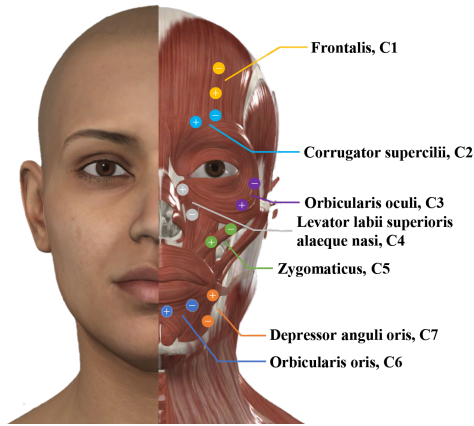


Fig. 2: Electrode distribution.

EMG signals based on the audio content. Specifically, we identified five key time points during the question and answer (Q&A) sessions:  $t_1$ ,  $t_2$ ,  $t_3$ , and  $t_4$ , representing the start and end of questions and answers, as shown in Fig. 3. These time points were used to extract the corresponding Q&A EMG signal segments. Subsequently, based on the true responses of the completed questionnaire, we labeled each Q&A EMG segment as truth-telling and lying.

Next, in order to analyze the EMG signal changes before, during and after lying, we subdivided each Q&A EMG signal segment into four phases, i.e., in-question (P1), pre-answer (P2), in-answer (P3) and post-answer (P4). The correspondence between the phases and the time periods are listed in Table 1.

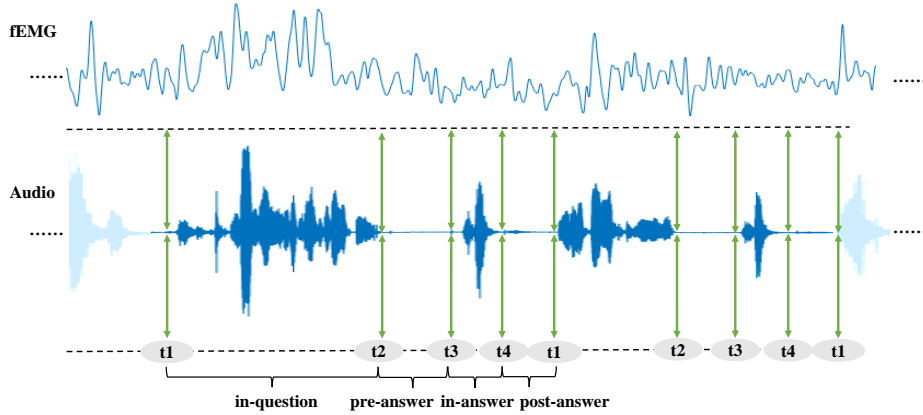


Fig. 3: Segmentation of the EMG signal through the time points obtained from the audio information.

Table 1: The phases correspond to specific time periods. The stage before truth-telling or lying includes the interrogee’s information-receiving phase (in-question, P1) and the preparation phase for answering (pre-answer, P2).  $t_{1N}$  denotes the start of the next Q&A session.

Index	Time	Phase	Label stage
P0	$t_1-t_{1N}$	whole Q&A	Truth-telling/Lying
P1	$t_1-t_2$	in-question	before Truth-telling/Lying
P2	$t_2-t_3$	pre-answer	during Truth-telling/Lying
P3	$t_3-t_4$	in-answer	during Truth-telling/Lying
P4	$t_4-t_{1N}$	post-answer	after Truth-telling/Lying

In addition, in order to eliminate the impact of the sequence effect on the subsequent analysis, we randomly shuffled the EMG signal segments of truth-telling and lying.

### 3.3 Data Pre-processing

After acquiring and segmenting the EMG signal, we performed pre-processing to address interference from direct current (DC) and noise present in the raw data. Additionally, individual differences led to varying EMG signal amplitudes across participants. The varying durations of each Q&A segment also required standardization to facilitate subsequent machine learning analysis.

**Signal Processing-Based EMG signal extraction** This subsection describes how to extract the specific EMG signals that reflect the facial muscle movements from the collected EMG raw data.

In the EMG acquisition process, the EMG device converts the electrical signal into a machine-analyzable digital signal after it is acquired. During this process, the DC would affect the EMG signals. Thus, we need to remove the DC offset at first. Specifically, the DC offset can be replaced by the mean value of the raw EMG signal  $x^{\text{raw}}$ , as shown in Eq. 1.

$$x_k^{\text{r-dc}} = x_k^{\text{raw}} - \frac{1}{n} \sum_{i=1}^n x_i^{\text{raw}} \quad (1)$$

where  $k \in [1, n]$ ,  $n$  represents the length of the EMG signal.  $x^{\text{r-dc}}$  represents the EMG signal after removing the DC offset.

To filter out noise and extract the EMG signal within the effective frequency band, we applied Butterworth filters, which are commonly used in EMG signal processing for their ability to preserve useful information. Specifically, due to the presence of 50 Hz power-line interference during the experiment, we set the cut-off frequencies of the bandstop Butterworth filter to 48 Hz and 52 Hz to eliminate the noise [28]. The filtered EMG signal,  $x^{\text{r-n}}$ , was obtained using Eq. 2.

$$x^{\text{r-n}} = \text{Butterworth}(x^{\text{r-dc}}, [48 \text{ Hz}, 52 \text{ Hz}], \text{stop}) \quad (2)$$

where  $\text{Butterworth}(u_1, u_2, u_3)$  is a bandpass or bandstop Butterworth filter. Specifically,  $u_1$  represents the input sequence;  $u_2$  indicates frequency range; and  $u_3$  represents type of filter (bandpass or bandstop).

Then, the cut-off frequency of the bandpass Butterworth filter on signal  $x^{\text{r-n}}$  was set to 20 Hz and 450 Hz for filtering the EMG signal  $x^{\text{f}}$  representing muscle movement [27].

$$x^{\text{f}} = \text{Butterworth}(x^{\text{r-n}}, [20 \text{ Hz}, 450 \text{ Hz}], \text{pass}) \quad (3)$$

The absolute value of  $x^{\text{f}}$  was retained for full-wave rectification, as shown in Eq. 4 (where  $\text{abs}(\cdot)$  denotes the absolute value operation). Since muscle activity is reflected in the amplitude variation of the EMG signal, we then applied an envelope to the signal, resulting in the final EMG signal analyzed in this study.

$$x^{\text{E}} = \text{Envelop}(\text{abs}(x^{\text{f}})) \quad (4)$$

where the operation  $\text{Envelop}(\cdot)$  returns the envelopes of the input sequence.

**Feature Construction** In this subsection, we focus on how to construct features for lie detection analysis based on EMG signals, including outlier removal, normalization and dimension reduction.

**Outlier removal:**

As we introduced in subsection 3.2, the EMG signals were segmented corresponding to each Q&A session. The duration of each EMG segment is different because the content length and the participants' speech tempo may vary across Q&A sessions. As illustrated in Fig. 4, the longest duration of the sample is 19.2 s, and the shortest is 1.3 s. To eliminate the impact of extreme length

on the analysis, we used the PauTa Criterion, i.e.,  $3\sigma$  Criterion [6], to remove abnormal samples, as shown in Eq. 5.

$$\mu = \frac{1}{N} \sum_{k=1}^N d_k, \quad \sigma = \sqrt{\frac{1}{N} \sum_{k=1}^N (d_k - \mu)^2} \quad (5)$$

where  $N$  denotes the total Q&A session amount,  $N = 1055$ ,  $d_k$  represents the  $k$ th sample duration.  $\mu$  and  $\sigma$  were calculated as the mean duration and the standard deviation. The sample duration outside the  $\mu \pm 3\sigma$  interval were considered as outliers and should be eliminated. Finally, 955 EMG signal segments were conserved for subsequent analysis. Furthermore, as previously described, we acquired EMG signal from seven channels simultaneously. Thus, for each EMG segment, there were seven channels of EMG signals.

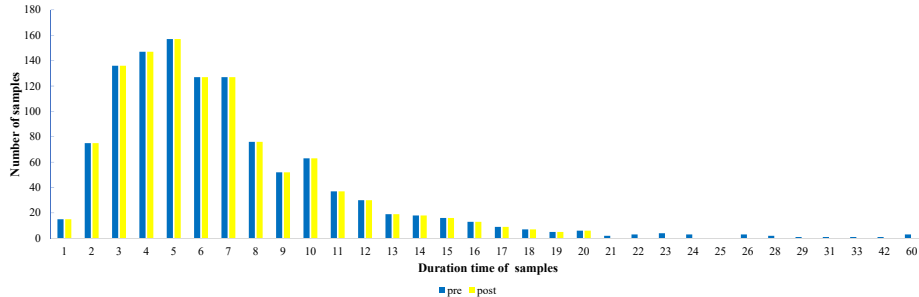


Fig. 4: EMG sample duration distribution.

### Normalization:

In the subsequent machine learning analysis, the model’s input features need to have a uniform length. To achieve this, we normalized the EMG segment lengths using linear Fast Fourier Transform (FFT) interpolation, with the longest sample as the baseline [18].

In this study, we not only analyzed lie detection using the overall EMG signal during the Q&A session (P0) but also examined the impact of EMG signals in different Q&A sub-phases. Based on Table 1, we performed interpolation normalization (Eqs. 6-7) for the whole session and its four phases: P0, P1, P2, P3, and P4. The resulting interpolated EMG features  $I$  are presented in Table 2.

$$p_{i,j} = \max[\text{len}(x_{i,1}^E), \dots, \text{len}(x_{i,6685}^E)] - \text{len}(x_{i,j}^E) \quad (6)$$

$$I_{i,j} = \text{interpft}(x_{i,j}^E, p_{i,j}) \quad (7)$$

Where  $i \in [1, 5]$  represents the entire segment and the four individual phases;  $j \in [1, 6685]$  corresponds to the 6685 EMG signal segments, with each segment

comprising seven channels of EMG signals. The functions  $\text{len}(\cdot)$ ,  $\text{max}[\cdot]$ , and  $\text{interpft}(\cdot)$  denote operations for calculating length, maximum value, and linear FFT interpolation, respectively.  $x_{i,j}^E$  represents the  $j$ th EMG signal of the  $i$ th phase,  $p_{i,j}$  is the number of interpolation points, and  $I_{i,j}$  represents the interpolated  $j$ th EMG feature of the  $i$ th phase.

Table 2: Interpolated EMG Feature Length for different Q&A phases.

Phase	P0	P1	P2	P3	P4
$I$ Length	14768	2823	1737	567	9641

**Dimension reduction:** The interpolated EMG features had high dimensionality, which could prolong the model training process and increase demands on computational resources. To mitigate this, we applied dimensionality reduction by removing irrelevant elements and retaining the most representative components for classification. Specifically, we used PCA to reduce feature dimensions, setting the retained energy value at 99.99

### 3.4 Machine Learning Methods

We aimed to verify whether computational algorithms can effectively learn features from EMG signals to detect lying. To assess learning efficiency, we compared two traditional machine learning models and one deep learning model.

Among the 955 EMG segments, 645 were truth-telling and 310 were lying, with consistent labeling across seven channels in each segment. Additionally, as shown in Eq. 8, EMG features from different phases were input into the models separately, enabling analysis of the importance of each phase for lie detection based on classification results.

$$Y_i^m = \text{Model}_m(X_i) \quad (8)$$

where  $i \in [1, 5]$ , indicates the whole and the four phases: P0, P1, P2, P3 and P4;  $m \in [1, 3]$ ,  $\text{Model}_m$  indicates the SVM, RUSBoost tree and ResNet, respectively.  $X_i$  and  $Y_i^m$  represent the input and output of the  $\text{Model}_m$ .

Notably, the traditional models use one-dimensional temporal EMG signals that have been interpolated and reduced in dimensionality. In contrast, the deep learning model utilizes two-dimensional spectrograms representing time-frequency domain changes in the EMG signal. To preserve frequency domain information, no interpolation or dimensionality reduction was applied to the EMG signal before generating the spectrograms.

**SVM (temporal domain).** For SVM, the input  $X_i$  is the interpolated and downsampled EMG feature  $F$ . Since uneven distribution of samples would affect the performance of the classifier, in addition to the experiment on all samples, we also conducted an experiment with the equal amounts of samples in both classes (lying and truth-telling).

**RUSBoosted tree (temporal domain).** For the RUSBoosted tree, which excels in handling unbalanced samples, we used all interpolated and downsampled EMG features  $F$  as input  $X_i$ . As shown in subsection 4.2, the RUSBoosted tree outperformed the other two models. Using this model, we classified lying and truth-telling based on the features of each EMG channel and various channel combinations. This approach allowed us to assess the relevance of muscle movements across different channels for lie detection.

**ResNet (time-frequency domain).** For the deep learning model, we selected ResNet, commonly used in image classification and target detection. Since ResNet requires a two-dimensional input, spectrograms were fed into the network. While deeper ResNet layers offer higher feature abstraction, they increase training time and slow convergence. To mitigate this, we employed transfer learning, initializing the model with parameters from a pre-trained ResNet34, ensuring fast and stable training. Spectrograms were scaled to  $256 \times 256$  pixels and center-cropped to  $224 \times 224$ . During training, a learning rate of 0.01 and a batch size of 16 were used. This configuration enhances training speed and accelerates convergence through parallel processing.

For evaluating classification results, we used 10-fold cross-validation. In this method, all features were divided into ten folds; nine were used for training, and one for testing. The model’s accuracy was calculated using Eq. 9, where lying and truth-telling are the positive and negative conditions, respectively.  $TP_n$  and  $TN_n$  represent the number of true positives (TPs) and true negatives (TNs) in the classification results. Additionally, we assessed the model’s performance using the AUC (area under the curve), providing a metric to measure the quality of the model’s predictions.

$$\text{Accuracy} = \frac{\sum_{n=1}^N (TP_n + TN_n)}{\text{Sample amount}} \quad (9)$$

## 4 Results and Discussion

### 4.1 Statistic Analysis

In this section, we separately introduced the results of lie detection by humans through visual face-to-face observation, as well as the statistical analysis results based on EMG.

After conducting statistical analysis, we discovered that the accuracy of human judges in differentiating between truth-telling and lying is 49.26%, which is essentially equivalent to random level. This outcome is in line with the majority of prior research [5]. Furthermore, we conducted a more detailed analysis of the accuracy in successful lie detection within the deceptive samples, which was found to be 33.86%, indicating a performance lower than the random level.

We analyzed the obtained EMG signal  $x^E$  using SPSS Statistics 26. First, we conducted Independent Sample T-Test on the truth-telling and lying samples in P0. As shown in Table 3, the results indicated that all channels were statistically

significant difference except for C5. Moreover, in C1, C2, and C7, the EMG during lying were significantly higher than truth-telling. Conversely, in C3, C4, and C6, the EMG during truth-telling were significantly higher than lying.

Table 3: Independent Samples T Test In P0 (Q&A session). M represents mean value; SD represents standard deviation value; \* represents  $p < 0.05$ . \*\* represents  $p < 0.01$ .

Channel	EMG(M± SD)		$t$	$p$
	truth-telling	lying		
C1	1.07±36.21	1.15±41.40	3.137	0.002**
C2	0.93±30.80	1.18±34.81	11.794	0.000**
C3	1.06±40.79	0.96±24.92	-5.528	0.000**
C4	1.05±35.03	0.86±26.14	-10.189	0.000**
C5	1.30±44.94	1.27±39.13	-1.095	0.274
C6	1.34±46.73	1.09±22.71	-12.184	0.000**
C7	1.18±43.25	1.45±45.03	9.872	0.000**

At the same time, we conducted participant-based analysis on the data in P0 using Paired Sample T-Test, which showed significant differences in C2 and C7. The EMG of C2 was significantly higher during lying (M= 1.38, SD= 2.27) than truth-telling (M= 0.79, SD= 1.63),  $t(15) = 2.33$ ,  $p = 0.03^*$  ( $p < 0.05$ ), and the EMG of C7 was also significantly higher during lying (M= 1.79, SD= 2.84) than truth-telling (M= 1.09, SD= 1.71),  $t(15) = 2.22$ ,  $p = 0.04^*$  ( $p < 0.05$ ).

## 4.2 Lie Detection Performance based on Machine learning

In this sub-section, we analyzed the performance of three EMG signal-based machine learning models for lie detection. Then, we explored the importance of different Q&A phases and facial muscles for lie detection.

**Model Performance** The Table 4 presented the accuracies and AUCs of the three models, i.e., SVM, RUSBoosted tree and ResNet.

The SVM model was tested with two input cases due to concerns about the impact of unbalanced sample distributions. The first case used all available samples for training and testing (SVM\_All), while the second used a balanced set of 310 lying and 310 truth-telling segments across 7 EMG channels (SVM\_Equal). SVM\_All achieved the highest accuracy, but its AUC was below 0.5, as shown in Fig. 5. SVM, being a nonlinear, high-dimensional model, performed well on the majority class, boosting overall accuracy. However, SVM’s sensitivity to data imbalance resulted in poor learning of the minority class (truth-telling), reflected in the low AUC. For SVM\_Equal, the balanced sample distribution reduced accuracy but improved AUC by decreasing the FPR.

Secondly, for RUSBoosted tree, it is able to handle the data imbalance well compared to SVM since it models the minority class better by removing the

Table 4: Performance comparison among SVM, RUSBoosted tree and the ResNet. The SVM has two types of sample inputs, one with all samples used for training and testing (All), and the other with an equal number of samples for lying and truth-telling (Equal). Acc represents Accuracy(%). The best results are highlighted in bold.

Models		P0		P1		P2		P3		P4	
		Acc	AUC	Acc	AUC	Acc	AUC	Acc	AUC	Acc	AUC
SVM	All	<b>67.2</b>	0.49±0.06	64.6	0.46±0.02	64.5	0.45±0.03	66.0	0.48±0.01	64.2	0.46±0.02
	Equal	56.0	<b>0.55±0.01</b>	53.6	0.51±0.03	53.7	0.52±0.02	55.5	0.53±0.01	54.3	0.52±0.01
RUSBoosted tree		<b>63.8</b>	<b>0.69±0.01</b>	60.5	0.64±0.02	60.0	0.63±0.01	62.1	0.68±0.01	61.2	0.65±0.01
ResNet		<b>61.0</b>	<b>0.66±0.01</b>	56.5	0.60±0.03	58.1	0.63±0.03	59.5	0.65±0.01	57.6	0.63±0.02

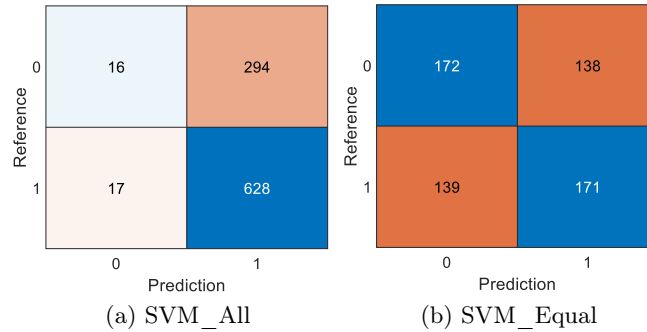


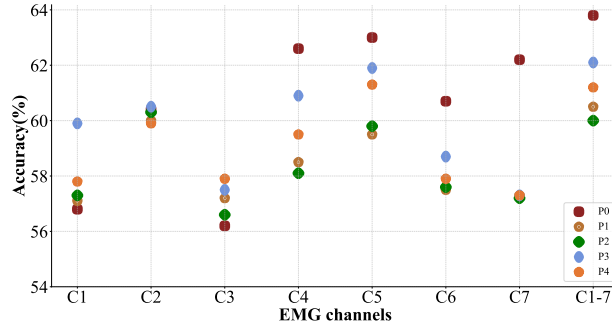
Fig. 5: Confusion matrix for SVM classifier with two input cases. 0 and 1 indicate the negative (truth-telling) and positive (lying) samples, respectively.

majority class samples. Therefore, it obtained the highest AUC value and the accuracy is moderately acceptable.

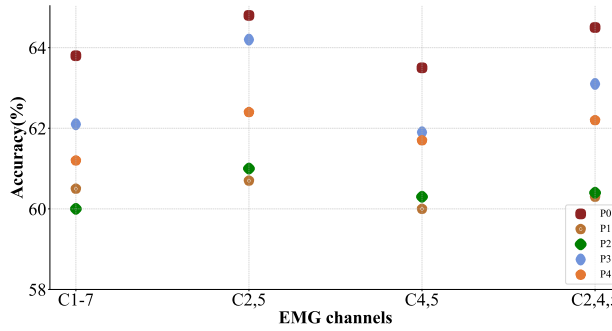
Finally, for the deep learning model, theoretically, the deep learning network is able to learn the features of the samples more deeply, and therefore should have better results. However, compared to traditional machine learning models, ResNet did not achieve the expected results. These results may be due to the small number of samples in our experiments, while ResNet usually requires a large amount of data for training.

**Importance of Different Q&A Phases for lie detection** Because RUS-Boosted tree classification had the best overall performance, we chose it for the subsequent analysis. Fig. 6 and Fig. 7 show the lie detection results of classifiers trained with EMG features from different muscle or muscle combinations under different Q&A phases.

From Table 4, Fig. 6 and Fig. 7, it can be seen that the overall phase P0 had the highest performance of lie detection because it contains the most information, i.e., the facial muscle movements during the whole Q&A session.



(a) Scatter plot shows lie detection performance in different phases with different EMG channels.



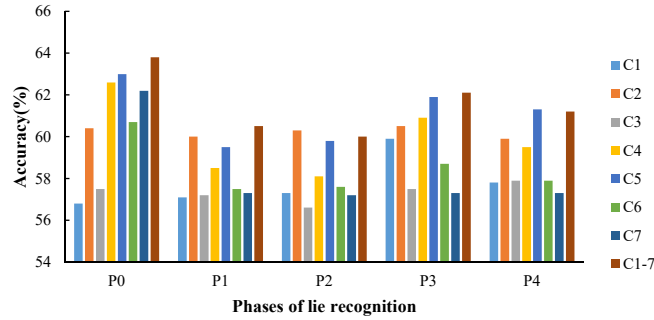
(b) Scatter plot shows lie detection performance in different phases with different EMG channel combinations.

Fig. 6: Lie detection comparison (Accuracy%) among different EMG channels and different Q&A phases - Scatter plots.

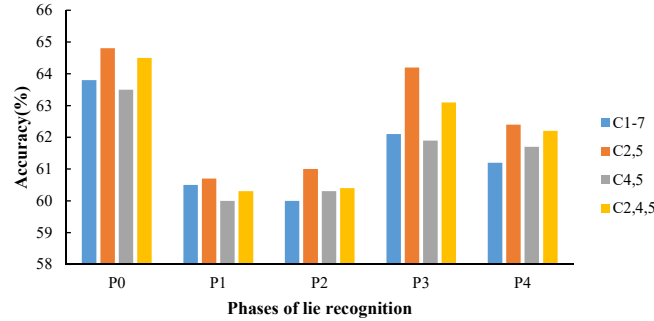
Specifically for the different phases of lie detection, the phase P3 had the best performance. This is because P3 corresponds to the phase of answering questions, which is the key stage when the interrogee express information to the interrogator and when facial movements are the most abundant. The features at this phase are the most discriminative, which is why the model is able to distinguish well between lying and truth-telling.

The performance of lie detection based on the P1 and P2 is the poorest. This two phases reflect the facial muscle movements of the interrogee before answering the question. The interrogees were more engaged in thinking rather than expressing. Therefore, the facial EMG in this phase contains the least action information.

For the P4, the facial movements in this phase are significantly reduced compared to P3. The EMG features of P4 may contain movements started at P3 that have not yet ended, or micro-expressions leaked without willing to be caught in a



(a) Histogram shows lie detection performance of different single EMG channels at different phases.



(b) Histogram shows lie detection performance of different EMG channel combinations at different phases.

Fig. 7: Lie detection comparison (Accuracy%) among different EMG channels and different Q&A phases - Histograms.

lie. The discrimination of these features is degraded. Therefore, the performance of lie detection based on P4 is lower than that of P3.

**Importance of Different Facial muscles for lie detection** Fig. 6 and Fig. 7 illustrate that for any of the Q&A phases, the lie detection performance is best when all channels of EMG features are fed into the model. This is because facial expressions tend to involve muscle actions in most regions of the face. When information from all channels is employed, the model is able to comprehensively learn the features relevant to lying.

Lie detection performance varied across EMG channels, with C2, C4, and C5 outperforming others. This aligns with the lie detection-related facial EMG regions identified by Dong et al. [8]. Movements in the corrugator supercillii (C2), levator labii superioris alaeque nasi (C4), and zygomaticus (C5) provided crucial cues for the model. Notably, the C7 channel, which tracks depressor anguli oris movements, showed a different accuracy trend across phases. While

C7 performed well in the overall phase P0—due to mouth movements providing verbal cues—its accuracy declined in sub-phases. This decline was due to limited mouth movements in phases P1, P2, and P4, and excessive interference from talking movements in phase P3.

Facial movements typically involve multiple muscles, not just single ones. To capture this complexity, we combined EMG features from channels C2, C4, and C5 in various permutations and used them as model inputs. The results, shown in Fig. 6b and 7b, indicate that the C2 and C5 combination achieved the highest accuracy, even surpassing the full-channel combination. This suggests that C2 and C5 provide the most relevant cues for detecting lies. Interestingly, adding more channels, like C2, C4, and C5 together, led to decreased model performance, implying that other channels may introduce noise rather than helpful information. These findings highlight the importance of focusing on Corrugator supercilii (C2) and Zygomaticus (C5) for lie detection using machine learning. Concentrating on these facial regions can enhance the accuracy and efficiency of models designed to detect lies based on physiological signals or visual data.

## 5 Conclusions

In our study, we showcased how statistics analysis and machine learning perform in recognizing intentional-deception. Statistics analysis provides some insights into the cognitive process of lying and the appearance of micro-expressions. Machine learning has revealed the different stages of lying and the importance of different facial muscles in lie detection. The integration of statistics analysis and machine learning has yielded valuable insights into the cognitive and physiological processes involved in lying. The experimental results also suggested that lie detection based on facial EMG signals can be an effective method for identifying deceptive behavior. Our study has shed light on the complex and multi-faceted nature of lying, and the challenges inherent in detecting deception. In addition, the potential for facial EMG signals to be used as a promising approach for future research in this area. As technology continues to advance, it is anticipated that the findings of this paper will contribute to the development of more sophisticated and accurate lie detection expert systems.

## Acknowledgements

This work is supported, in part, by grants from the National Natural Science Foundation of China (62276252, 62106256), in part, by Research on the construction of social psychological service system for teenagers in the new era(23BSHJ01), and in part, by a grant from the Youth Innovation Promotion Association CAS.

## References

1. Ang, L.B.P., Belen, E.F., Bernardo, R.A., Boongaling, E.R., Briones, G.H., Coronel, J.B.: Facial expression recognition through pattern analysis of facial muscle

- movements utilizing electromyogram sensors. In: 2004 IEEE Region 10 Conference TENCN 2004. vol. 100, pp. 600–603. IEEE (2004)
2. Bishop, C.M., Nasrabadi, N.M.: Pattern recognition and machine learning, vol. 4. Springer (2006)
  3. Blair, J.P., Levine, T.R., Shaw, A.S.: Content in context improves deception detection accuracy. *Human Communication Research* **36**(3), 423–442 (2010)
  4. Bond, G.D.: Deception detection expertise. *Law and Human Behavior* **32**(4), 339–351 (2008)
  5. Bond Jr, C.F., DePaulo, B.M.: Accuracy of deception judgments. *Personality and social psychology Review* **10**(3), 214–234 (2006)
  6. Chandola, V., Banerjee, A., Kumar, V.: Anomaly detection for discrete sequences: A survey. *IEEE transactions on knowledge and data engineering* **24**(5), 823–839 (2010)
  7. DePaulo, B.M., Kashy, D.A., Kirkendol, S.E., Wyer, M.M., Epstein, J.A.: Lying in everyday life. *Journal of personality and social psychology* **70**(5), 979–995 (1996)
  8. Dong, Z., Wang, G., Lu, S., Li, J., Yan, W., Wang, S.J.: Spontaneous facial expressions and micro-expressions coding: From brain to face. *Frontiers in Psychology* p. 5808 (2022)
  9. Dopson, W.G., Beckwith, B.E., Tucker, D.M., Bullard-Bates, P.C.: Asymmetry of facial expression in spontaneous emotion. *Cortex* **20**(2), 243–251 (1984)
  10. Edelstein, R.S., Luten, T.L., Ekman, P., Goodman, G.S.: Detecting lies in children and adults. *Law and Human Behavior* **30**(1), 1–10 (2006)
  11. Ekman, P.: Darwin, deception, and facial expression. *Annals of the new York Academy of sciences* **1000**(1), 205–221 (2003)
  12. Ekman, P., Friesen, W.V.: Nonverbal leakage and clues to deception. *Psychiatry* **32**(1), 88–106 (1969)
  13. Fricke, C., Alizadeh, J., Zakhary, N., Woost, T.B., Bogdan, M., Classen, J.: Evaluation of three machine learning algorithms for the automatic classification of emg patterns in gait disorders. *Frontiers in neurology* **12**, 666458 (2021)
  14. Girouard, M., Cavazos, J.E.: Electromyography-based seizure detector: Preliminary results comparing a generalized tonic-clonic seizure detection algorithm to video-eeg recordings. *Epilepsia* **56**(9), 1432–1437 (2015)
  15. Güler, N.F., Koçer, S.: Classification of emg signals using pca and fft. *Journal of medical systems* **29**, 241–250 (2005)
  16. Hurley, C.M., Anker, A.E., Frank, M.G., Matsumoto, D., Hwang, H.C.: Background factors predicting accuracy and improvement in micro expression recognition. *Motivation and emotion* **38**, 700–714 (2014)
  17. Joshi, D., Nakamura, B.H., Hahn, M.E.: High energy spectrogram with integrated prior knowledge for EMG-based locomotion classification. *Medical Engineering & Physics* **37**(5), 518–524 (2015)
  18. Kim, H., Zhang, D., Kim, L., Im, C.H.: Classification of individual’s discrete emotions reflected in facial microexpressions using electroencephalogram and facial electromyogram. *Expert Systems with Applications* **188**, 116101 (2022)
  19. Levine, T.R.: New and improved accuracy findings in deception detection research. *Current Opinion in Psychology* **6**, 1–5 (2015)
  20. Li, J., Dong, Z., Lu, S., Wang, S.J., Yan, W.J., Ma, Y., Liu, Y., Huang, C., Fu, X.: CAS(ME)<sup>3</sup>: A third generation facial spontaneous micro-expression database with depth information and high ecological validity. *IEEE Transactions on Pattern Analysis and Machine Intelligence* **45**(3), 2782–2800 (2023)

21. Luo, M., Hancock, J.T., Markowitz, D.M.: Credibility perceptions and detection accuracy of fake news headlines on social media: Effects of truth-bias and endorsement cues. *Communication Research* **49**(2), 171–195 (2022)
22. Mac Giolla, E., Luke, T.J.: Does the cognitive approach to lie detection improve the accuracy of human observers? *Applied Cognitive Psychology* **35**(2), 385–392 (2021)
23. Owayjan, M., Kashour, A., Al Haddad, N., Fadel, M., Al Souki, G.: The design and development of a lie detection system using facial micro-expressions. In: 2012 2nd international conference on advances in computational tools for engineering applications (ACTEA). pp. 33–38. IEEE (2012)
24. Ozdemir, M.A., Kisa, D.H., Guren, O., Onan, A., Akan, A.: EMG based hand gesture recognition using deep learning. In: 2020 Medical Technologies Congress (TIPTEKNO). pp. 1–4. IEEE (2020)
25. O’Sullivan, M.: Emotional intelligence and deception detection: Why most people can’t “read” others, but a few can. *Applications of nonverbal communication* pp. 215–253 (2005)
26. Porter, S., Ten Brinke, L., Wallace, B.: Secrets and lies: Involuntary leakage in deceptive facial expressions as a function of emotional intensity. *Journal of Nonverbal Behavior* **36**(1), 23–37 (2012)
27. Reaz, M., Hussain, M.S., Mohd-Yasin, F.: Techniques of emg signal analysis: detection, processing, classification and applications. *Biological Procedures Online* **8**(1), 11–35 (2006)
28. Sarwar, N., Sandhu, M.S., Ricketts, S.L., Butterworth, A.S., et al.: Triglyceride-mediated pathways and coronary disease: collaborative analysis of 101 studies. *The Lancet* **375**(9726), 1634–1639 (2010)
29. Seiffert, C., Khoshgoftaar, T.M., Van Hulse, J., Napolitano, A.: Rusboost: A hybrid approach to alleviating class imbalance. *IEEE Transactions on Systems, Man, and Cybernetics-Part A: Systems and Humans* **40**(1), 185–197 (2009)
30. Shuster, A., Inzelberg, L., Ossmy, O., Izakson, L., Hanein, Y., Levy, D.J.: Lie to my face: An electromyography approach to the study of deceptive behavior. *Brain and Behavior* **11**(12), e2386 (2021)
31. Srivastava, N., Dubey, S.: Deception detection using artificial neural network and support vector machine. In: 2018 Second International Conference on Electronics, Communication and Aerospace Technology (ICECA). pp. 1205–1208. IEEE (2018)
32. Ten Brinke, L., Lee, J.J., Carney, D.R.: Different physiological reactions when observing lies versus truths: Initial evidence and an intervention to enhance accuracy. *Journal of personality and social psychology* **117**(3), 560–578 (2019)
33. Vrij, A., Granhag, P.A., Porter, S.: Pitfalls and opportunities in nonverbal and verbal lie detection. *Psychological science in the public interest* **11**(3), 89–121 (2010)
34. Wagner-Altendorf, T.A., Van der Lugt, A.H., Banfield, J.F., Meyer, C., Rohrbach, C., Heldmann, M., Münte, T.F.: The electrocortical signature of successful and unsuccessful deception in a face-to-face social interaction. *Frontiers in Human Neuroscience* **14**, 277 (2020)
35. Zawawi, T.T., Abdullah, A.R., Shair, E.F., Halim, I., Rawaida, O.: Electromyography signal analysis using spectrogram. In: 2013 IEEE Student Conference on Research and Development. pp. 319–324. IEEE (2013)